Oz, M. C., Hicklin, D. J., Witte, L., Moore, M. A., and Rafii, S. (2000) *Blood* **95,** 952–958
9. Rehman, J., Li, J., Orschell, C. M., and March, K. L. (2003) *Circulation* **107,** 1164–1169
10. Kocher, A. A., Schuster, M. D., Szabolcs, M. J., Takuma, S., Burkhoff, D., Wang, J., Homma, S., Edwards, N. M., and Itescu, S. (2001) *Nat. Med.* **7,** 430–436
11. Bahlmann, F. H., De Groot, K., Spandau, J. M., Landry, A. L., Hertel, B., Duckert, T., Boehm, S. M., Menne, J., Haller, H., and Fliser, D. (2004) *Blood* **103,** 921–926
12. Bahlmann, F. H., DeGroot, K., Duckert, T., Niemczyk, E., Bahlmann, E., Boehm, S. M., Haller, H., and Fliser, D. (2003) *Kidney Int.* **64,** 1648–1652
13. Heeschen, C., Aicher, A., Lehmann, R., Fichtlscherer, S., Vasa, M., Urbich, C., Mildner-Rihm, C., Martin, H., Zeiher, A. M., and Dimmeler, S. (2003) *Blood* **102,** 1340–1346
14. Dimmeler, S., Aicher, A., Vasa, M., Mildner-Rihm, C., Adler, K., Tiemann, M., Rutten, H., Fichtlscherer, S., Martin, H., and Zeiher, A. M. (2001) *J. Clin. Investig.* **108,** 391–397
15. Llevadot, J., Murasawa, S., Kureishi, Y., Uchida, S., Masuda, H., Kawamoto, A., Walsh, K., Isner, J. M., and Asahara, T. (2001) *J. Clin. Investig.* **108,** 399–405
16. Kaushansky, K., Lok, S., Holly, R. D., Broudy, V. C., Lin, N., Bailey, M. C., Forstrom, J. W., Buddle, M. M., Oort, P. J., Hagen, F. S., Roth, G. J., Papayannopoulou, T., and Foster, D. C. (1994) *Nature* **369,** 568–571
17. Fox, N., Priestley, G., Papayannopoulou, T., and Kaushansky, K. (2002) *J. Clin. Investig.* **110,** 389–394
18. Kimura, S., Roberts, A. W., Metcalf, D., and Alexander, W. S. (1998) *Proc. Natl. Acad. Sci. U. S. A.* **95,** 1195–1200
19. Sitnicka, E., Lin, N., Priestley, G. V., Fox, N., Broudy, V. C., Wolf, N. S., and Kaushansky, K. (1996) *Blood* **87,** 4998–5005
20. Brizzi, M. F., Battaglia, E., Montrucchio, G., Dentelli, P., Del Sorbo, L., Garbarino, G., Pegoraro, L., and Camussi, G. (1999) *Circ. Res.* **84,** 785–796
21. Kaushansky, K., Lin, N., Grossmann, A., Humes, J., Sprugel, K. H., and Broudy, V. C. (1996) *Exp. Hematol.* **24,** 265–269
22. Broudy, V. C., Lin, N. L., and Kaushansky, K. (1995) *Blood* **85,** 1719–1726
23. Kaushansky, K., Broudy, V. C., Grossmann, A., Humes, J., Lin, N., Ren, H. P., Bailey, M. C., Papayannopoulou, T., Forstrom, J. W., and Sprugel, K. H. (1995) *J. Clin. Investig.* **96,** 1683–1687
24. Kobayashi, M., Laver, J. H., Kato, T., Miyazaki, H., and Ogawa, M. (1995) *Blood* **86,** 2494–2499
25. Kanayasu-Toyoda, T., Yamaguchi, T., Oshizawa, T., and Hayakawa, T. (2003) *J. Cell. Physiol.* **195,** 119–129
26. Hur, J., Yoon, C. H., Kim, H. S., Choi, J. H., Kang, H. J., Hwang, K. K., Oh, B. H., Lee, M. M., and Park, Y. B. (2004) *Arterioscler. Thromb. Vasc. Biol.* **24,** 288–293
27. Yoon, C. H., Hur, J., Park, K. W., Kim, J. H., Lee, C. S., Oh, I. Y., Kim, T. Y., Cho, H. J., Kang, H. J., Chae, I. H., Yang, H. K., Oh, B. H., Park, Y. B., and Kim, H. S. (2005) *Circulation* **112,** 1618–1627
28. Miyakawa, Y., Rojnuckarin, P., Habib, T., and Kaushansky, K. (2001) *J. Biol. Chem.* **276,** 2494–2502
29. Drachman, J. G., Sabath, D. F., Fox, N. E., and Kaushansky, K. (1997) *Blood* **89,** 483–492
30. Kirito, K., Watanabe, T., Sawada, K., Endo, H., Ozawa, K., and Komatsu, N. (2002) *J. Biol. Chem.* **277,** 8329–8337
31. Li, A., Dubey, S., Varney, M. L., Dave, B. J., and Singh, R. K. (2003) *J. Immunol.* **170,** 3369–3376
32. Mizukami, Y., Jo, W. S., Duerr, E. M., Gala, M., Li, J., Zhang, X., Zimmer, M. A., Iliopoulos, O., Zukerberg, L. R., Kohgo, Y., Lynch, M. P., Rueda, B. R., and Chung, D. C. (2005) *Nat. Med.* **11,** 992–997
33. Salcedo, R., Ponce, M. L., Young, H. A., Wasserman, K., Ward, J. M., Kleinman, H. K., Oppenheim, J. J., and Murphy, W. J. (2000) *Blood* **96,** 34–40
34. Lin, Y., Weisdorf, D. J., Solovey, A., and Hebbel, R. P. (2000) *J. Clin. Investig.* **105,** 71–77
35. Assmus, B., Schachinger, V., Teupe, C., Britten, M., Lehmann, R., Dobert, N., Grunwald, F., Aicher, A., Urbich, C., Martin, H., Hoelzer, D., Dimmeler, S., and Zeiher, A. M. (2002) *Circulation* **106,** 3009–3017
36. Kalka, C., Masuda, H., Takahashi, T., Kalka-Moll, W. M., Silver, M., Kearney, M., Li, T., Isner, J. M., and Asahara, T. (2000) *Proc. Natl. Acad. Sci. U. S. A.* **97,** 3422–3427
37. Kawamoto, A., Gwon, H. C., Iwaguro, H., Yamaguchi, J. I., Uchida, S., Masuda, H., Silver, M., Ma, H., Kearney, M., Isner, J. M., and Asahara, T. (2001) *Circulation* **103,** 634–637
38. Kirito, K., Fox, N., Komatsu, N., and Kaushansky, K. (2005) *Blood* **105,** 4258–4263
39. Kelemen, E., Cserhati, I., and Tanos, B. (1958) *Acta Haematol. (Basel)* **20,** 350–355
40. Yamamoto, S. (1957) *Acta Haematol. Jpn.* **20,** 163
41. Kanayasu-Toyoda, T., Yamaguchi, T., Uchida, E., and Hayakawa, T. (1999) *J. Biol. Chem.* **274,** 25471–25480
42. Yamaguchi, T., Mukasa, T., Uchida, E., Kanayasu-Toyoda, T., and Hayakawa, T. (1999) *J. Biol. Chem.* **274,** 15575–15581
43. Miyamoto, K., Nishigami, K., Nagaya, N., Akutsu, K., Chiku, M., Kamei, M., Soma, T., Miyata, S., Higashi, M., Tanaka, R., Nakatani, T., Nonogi, H., and Takeshita, S. (2006) *Circulation* **114,** 2679–2684
44. George, J., Afek, A., Abashidze, A., Shmilovich, H., Deutsch, V., Kopolovich, J., Miller, H., and Keren, G. (2005) *Arterioscler. Thromb. Vasc. Biol.* **25,** 2636–2641

# Miscibility of Nifedipine and Hydrophilic Polymers as Measured by $^1$H-NMR Spin–Lattice Relaxation

Yukio Aso,*[a] Sumie Yoshioka,[a] Tamaki Miyazaki,[a] Tohru Kawanishi,[a] Kazuyuki Tanaka,[b] Satoshi Kitamura,[b] Asako Takakura,[c] Takashi Hayashi,[c] and Noriyuki Muranushi[c]

[a] *National Institute of Health Sciences; 1–18–1 Kamiyoga, Setagaya-ku, Tokyo 158–8501, Japan:* [b] *Astellas Pharma Inc.; 180 Ozumi, Yaizu, Shizuoka 425–0072, Japan: and* [c] *Shionogi & Co., Ltd.; 2–1–3 Kuise, Terajima, Amagasaki, Hyogo 660–0813, Japan.* Received April 19, 2007; accepted June 4, 2007; published online June 5, 2007

**The miscibility of a drug with excipients in solid dispersions is considered to be one of the most important factors for preparation of stable amorphous solid dispersions. The purpose of the present study was to elucidate the feasibility of $^1$H-NMR spin–lattice relaxation measurements to assess the miscibility of a drug with excipients. Solid dispersions of nifedipine with the hydrophilic polymers poly(vinylpyrrolidone) (PVP), hydroxypropylmethylcellulose (HPMC) and α,β-poly(*N*-5-hydroxypentyl)-L-aspartamide (PHPA) with various weight ratios were prepared by spray drying, and the spin–lattice relaxation decay of the solid dispersions in a laboratory frame ($T_1$ decay) and in a rotating frame ($T_{1\rho}$ decay) were measured. $T_{1\rho}$ decay of nifedipine–PVP solid dispersions (3 : 7, 5 : 5 and 7 : 3) was describable with a mono-exponential equation, whereas $T_{1\rho}$ decay of nifedipine–PHPA solid dispersions (3 : 7, 4 : 6 and 5 : 5) was describable with a bi-exponential equation. Because a mono-exponential $T_{1\rho}$ decay indicates that the domain sizes of nifedipine and polymer in solid dispersion are less than several nm, it is speculated that nifedipine is miscible with PVP but not miscible with PHPA. All the nifedipine–PVP solid dispersions studied showed a single glass transition temperature ($T_g$), whereas two glass transitions were observed for the nifedipine–PHPA solid dispersion (3 : 7), thus supporting the above speculation. For nifedipine–HPMC solid dispersions (3 : 7 and 5 : 5), the miscibility of nifedipine and HPMC could not be determined by DSC measurements due to the lack of obviously evident $T_g$. In contrast, $^1$H-NMR spin–lattice relaxation measurements showed that nifedipine and HPMC are miscible, since $T_{1\rho}$ decay of the solid dispersions (3 : 7, 5 : 5 and 7 : 3) was describable with a mono-exponential equation. These results indicate that $^1$H-NMR spin–lattice relaxation measurements are useful for assessing the miscibility of a drug and an excipient in solid dispersions.**

**Key words** miscibility; solid dispersion; spin diffusion; spin–lattice relaxation time; amorphous

Preparing solid dispersions of a poorly soluble drug with water-soluble polymers is a promising method for improving the dissolution characteristics and bioavailability of the drug. Miscibility between a drug and a polymer is considered to be one of the most important factors for obtaining stable solid dispersions.[1)]

Miscibility of a drug with a polymer is usually evaluated by differential scanning calorimetry (DSC).[2—6)] When a solid dispersion shows a single glass transition temperature ($T_g$) between the $T_g$ values of the drug and the polymer, the drug and the polymer are considered to be miscible within the detection limit of DSC.[7)] This method is applicable to a solid dispersion when $T_g$ of the drug and the polymer can be detected clearly, and the temperature ranges of the base line shift due to glass transition do not overlap each other.

The interaction parameter $\chi$ of the Flory–Huggins equation provides a measure of miscibility.[8,9)] Crowly and Zografi measured the water vapor sorption isotherm of indomethacin solid dispersions with PVP and reported that the estimated interaction parameter $\chi$ between indomethacin and PVP was greater than 0.5, indicating that indomethacin and PVP are immiscible in terms of $\chi$ value.[8)] Although this method is excellent in being able to provide a quantitative measure of miscibility, it may be difficult to apply to unstable amorphous drugs, which crystallize during measurement of water vapor sorption.

A method that can be used as an alternative to DSC or measurement of the interaction parameter $\chi$ is analysis of the $^1$H spin–lattice relaxation process of solid dispersions, which has been reported in the fields of polymer alloy and polymer blends. If two polymers are miscible, the relaxation decay of the mixture is describable by a mono-exponential equation, whereas if they are not miscible, relaxation decay is describable by a bi-exponential equation.[10,11)]

In this paper, the feasibility of $^1$H spin–lattice relaxation measurements for evaluating the miscibility of a drug and polymers in solid dispersions was studied. Nifedipine solid dispersions with PVP, HPMC and α,β-poly(*N*-5-hydroxypentyl)-L-aspartamide (PHPA) were used as model solid dispersions, and the miscibility measured by $^1$H-NMR was compared with that measured by DSC. The dissolution profiles of nifedipine from PVP solid dispersions were compared with those from PHPA solid dispersions to discuss the effects of miscibility on the dissolution rate of nifedipine.

**Theory** $^1$H spin–lattice relaxation rates of respective spins in a solid are usually averaged by a process called spin diffusion. Spin diffusion is the equilibration process of polarizations of spins at different local sites through mutual exchange of magnetization. $^1$H spin–lattice relaxation decay for a single-phase solid is describable by a mono-exponential equation with a relaxation rate that is averaged by spin diffusion. When a solid consists of two phases, the spin–lattice relaxation decay is describable by a mono-exponential or a bi-exponential equation depending on both the domain size of each phase and the effective diffusion length ($L$). $L$ is expressed as follows:

$$L=\sqrt{6Dt} \quad (1)$$

* To whom correspondence should be addressed. e-mail: aso@nihs.go.jp

where $D$ is the spin diffusion coefficient, and $t$ is the diffusion time. $D$ is a function of the distance between neighboring proton spins and spin–spin relaxation time ($T_2$), and is reported to be approximately $10^{-12}$ cm$^2$ s$^{-1}$ for organic polymers. Typical spin–lattice relaxation time in a laboratory frame ($T_1$) and that in a rotating frame ($T_{1\rho}$) are of the order of 1 s and 10 ms, respectively. When these values for $t$ were inserted in Eq. 1, effective diffusion lengths of approximately 50 nm and 5 nm were obtained for $T_1$ and $T_{1\rho}$, respectively. Depending on the domain size of each phase in a solid, the following 3 cases can be expected: (1) when the domain is smaller than about 5 nm, both the spin–lattice relaxation decay patterns in a laboratory frame ($T_1$ decay) and in a rotating frame ($T_{1\rho}$ decay) are describable by a mono-exponential equation; (2) when the domain size is about 5 to 50 nm, the $T_{1\rho}$ decay pattern is describable by a bi-exponential equation, whereas the $T_1$ decay pattern is describable by a mono-exponential equation; and (3) when the domain size is larger than about 50 nm, both the $T_1$ and $T_{1\rho}$ decay patterns are describable by a bi-exponential equation. When the $T_{1\rho}$ decay is describable by a mono-exponential equation, the solid can be considered as a single phase within the detection limit of NMR. $T_1$ and $T_{1\rho}$ decay thus provide information on miscibility of a drug and a polymer excipient.[11]

## Experimental

**Materials** Nifedipine (N-7634), PVP (PVP-40) and HPMC (H-3785) were purchased from Sigma (Newcastle, DE, U.S.A.). PHPA was synthesized *via* polycondensation of L-aspartic acid.[12] Phenobarbital was obtained from sodium phenobarbital (Wako Pure Chemical Ind., Osaka) by neutralization and subsequent re-crystallization from acetone solutions as described previously.[13] Other chemicals used were of reagent grade. Nifedipine solid dispersions with PVP, HPMC and PHPA were prepared by a solvent evaporation method using a model GS-310 spray dryer (Yamato, Tokyo, Japan). Drying conditions are summarized in Table 1. The solid dispersions obtained were confirmed to be amorphous from microscopic observation under polarized light. Although the drying conditions were not optimized, 50 to 90% of the solid dispersions were obtained. Amorphous nifedipine was prepared by melting and subsequent rapid cooling as reported previously.[14]

**DSC** $T_g$ of nifedipine–PVP and nifedipine–HPMC solid dispersions was measured by modulated temperature DSC using a model 2920 differential scanning calorimeter and a refrigerator cooling system (TA Instruments, Newcastle, DE, U.S.A.). The modulated temperature program used was a modulation amplitude of ±0.5 °C, a modulation period of 100 s and an underlying heating rate of 1 °C/min. For nifedipine–PHPA solid dispersions, $T_g$ was measured at a scanning rate of 20 °C/min using a conventional heating program. Temperature calibration of the instrument was carried out using indium.

**NMR** $T_1$ decay and $T_{1\rho}$ decay were measured using a model JNM-MU25 pulsed NMR spectrometer (JEOL DATUM, Tokyo, Japan). The inversion recovery pulse sequence was used to measure $T_1$ decay. $T_{1\rho}$ decay was measured in a spin locking field of 10 G. All measurements were carried out at 27 °C.

**X-Ray Powder Diffraction** X-Ray powder diffraction patterns of solid dispersions were obtained using a model RINT-TTR II X-ray diffractometer (Rigaku Denki, Tokyo) with Cu$K\alpha$ radiation (50 kV, 300 mA) at a scanning rate of 4 °C/min from $2\theta = 5°$ to 40°.

**Nifedipine Dissolution Profile** Nifedipine–PVP (3 : 7) and nifedipine–PHPA (3 : 7) solid dispersions containing 100 mg of nifedipine were made into disks with a diameter of 2 cm at a pressure of 20 kN. Each disk was mounted on the rotor of the dissolution apparatus and the side surface of the disk was covered with a Teflon film. The sample was rotated at a rate of 100 rpm in 900 ml of distilled water at 37 °C. The amount of nifedipine dissolved was measured using a model DM-3100 solution monitor (Otsuka Electronics, Tokyo).

## Results and Discussion

Figure 1 shows typical $T_1$ and $T_{1\rho}$ decay patterns for the solid dispersion and the physical mixture of nifedipine and PHPA (3 : 7). $T_1$ and $T_{1\rho}$ decay patterns were mono-exponential for both amorphous nifedipine and PHPA. The $T_1$ and $T_{1\rho}$ values of nifedipine were 5.0 s and 104 ms, respectively, and those of PHPA were 0.084 s and 4.4 ms, respectively. The physical mixture of nifedipine and PHPA (3 : 7) exhibited bi-exponential $T_1$ and $T_{1\rho}$ decay with the relaxation time of each component, indicating that the particle sizes of nifedipine and PHPA in the physical mixture are much larger than the effective diffusion length (approximately 5 nm and 50 nm for $T_{1\rho}$ and $T_1$ decay, respectively). In contrast to the physical

Table 1. Conditions of Spray Drying

| Drug | Polymer | Solvent[a] | Outlet temperature (°C) | Atomizer gas (l/min) | Feeding rate (ml/min) |
|---|---|---|---|---|---|
| Nifedipine–PHPA | | | | | |
| 0 | 10 | A | 68 | 7 | 5 |
| 3 | 7 | A | 68 | 7 | 3 |
| 4 | 6 | A | 68 | 7 | 3 |
| 5 | 5 | A | 68 | 7 | 3 |
| Phenobarbital–PHPA | | | | | |
| 3 | 7 | A | 68 | 7 | 3 |
| Nifedipine–PVP | | | | | |
| 0 | 10 | A | 90 | 9 | 10 |
| 3 | 7 | A | 90 | 9 | 10 |
| 5 | 5 | A | 90 | 9 | 10 |
| 7 | 3 | A | 68 | 7 | 3 |
| Nifedipine–HPMC | | | | | |
| 0 | 10 | B | 38 | 11 | 3 |
| 3 | 7 | B | 38 | 11 | 2 |
| 5 | 5 | B | 38 | 11 | 2 |
| 7 | 3 | B | 38 | 11 | 4 |

*a*) Solvent A, ethanol; solvent B, ethanol–$CH_2Cl_2$ (1 : 1). Flow rate of drying gas was adjusted to 0.5 m$^3$/min.

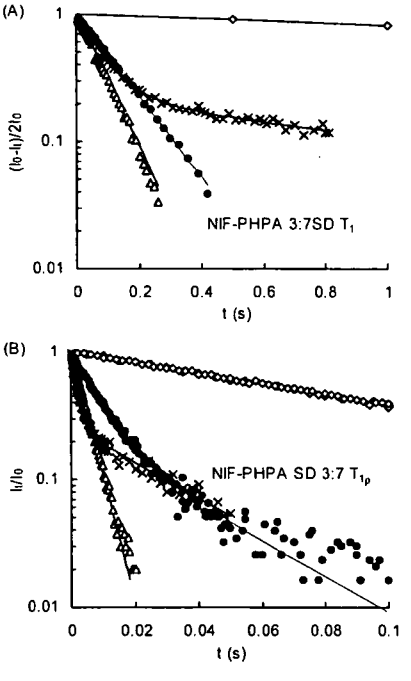


Fig. 1. $T_1$ (A) and $T_{1\rho}$ (B) Decay Patterns for Amorphous Nifedipine (◇), Amorphous PHPA (△), Physical Mixture (×) and Solid Dispersions (●) of Nifedipine and PHPA

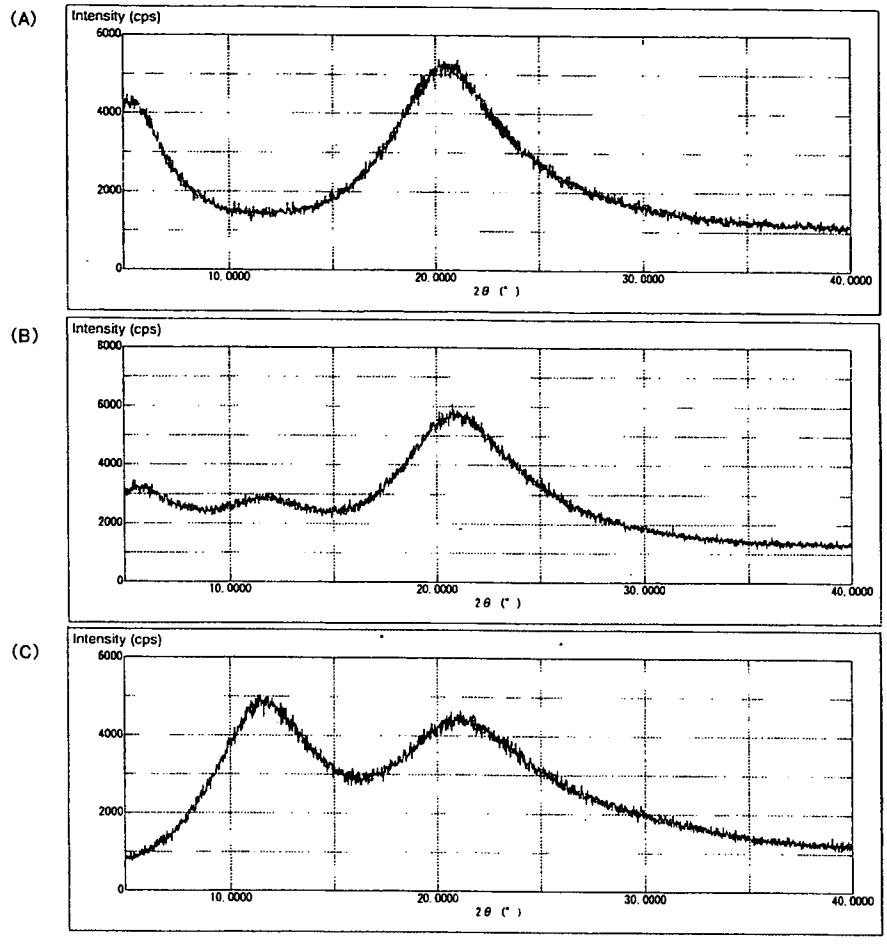


Fig. 2. Powder X-Ray Diffraction Patterns of PHPA (A), Nifedipine–PHPA (3 : 7) (B) and Nifedipine–PVP Solid Dispersions (3 : 7) (C)

mixture, the solid dispersion (3 : 7) showed mono-exponential $T_1$ decay, whereas bi-exponential $T_{1\rho}$ decay. These results indicate that nifedipine and PHPA are immiscible and that domains 5 to 50 nm in size are present in the solid dispersion. The nifedipine–PHPA solid dispersions (4 : 6 and 5 : 5) and the phenobarbital–PHPA solid dispersions (3 : 7) also exhibited bi-exponential $T_{1\rho}$ decay (data not shown). Figure 2 shows powder X-ray diffraction patterns of the nifedipine–PHPA and nifedipine–PVP solid dispersions. The observed halo pattern indicates that nifedipine in the PHPA dispersions is amorphous at the detection limit of powder X-ray diffractometry.

DSC data supported the contention that nifedipine and PHPA are immiscible. Figure 3 shows typical DSC traces for nifedipine–PHPA solid dispersions. The nifedipine–PHPA solid dispersion (3 : 7) showed glass transition at approximately 50 °C, corresponding to the $T_g$ of amorphous nifedipine, and at approximately 75 °C, indicating that there are both an amorphous nifedipine phase and an amorphous nifedipine–PHPA phase in the solid dispersion. These DSC data indicate that amorphous nifedipine and PHPA are partially immiscible at this weight ratio. For the nifedipine–PHPA solid dispersion (5 : 5), $T_g$ of the amorphous nifedipine–PHPA phase was not clearly observed because of the detection limit of DSC, suggesting that $^1$H-NMR relaxation measurements can detect immiscibility of drugs and polymers more sensitively than DSC. DSC data suggest that the nifedipine–PHPA solid dispersion (3 : 7) consists of pure amorphous nifedipine phase and amorphous nifedipine–PHPA phase. NMR data may support this speculation. As shown in Fig. 1B, initial $T_{1\rho}$ decay of the solid dispersion was slower than that of the physical mixture or pure PHPA. This slow relaxation rate of the solid dispersion may indicate that the relaxation rate of PHPA protons was decreased by spin diffusion with nifedipine protons existing near PHPA molecules; in other words, nifedipine–PHPA phase is considered to exist in the solid dispersion. The effect of weight ratios on the $T_{1\rho}$ decay of nifedipine–PHPA solid dispersions needs to examine in order

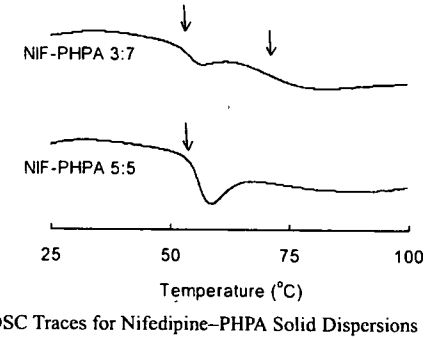


Fig. 3. DSC Traces for Nifedipine–PHPA Solid Dispersions
Arrows represent $T_g$.

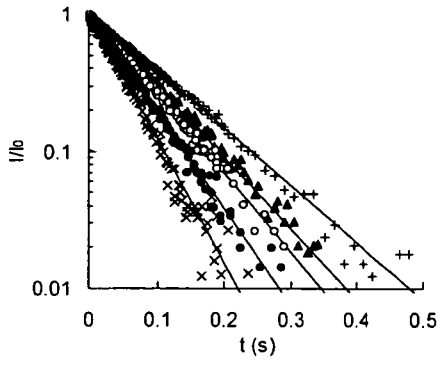


Fig. 4. $T_{1\rho}$ Decay Patterns for Nifedipine (+), PVP (×), and Nifedipine–PVP Solid Dispersions of 7 : 3 (▲), 5 : 5 (○), and 3 : 7 (●)

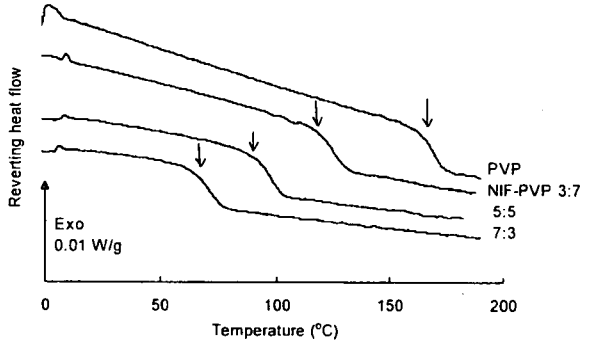


Fig. 5. DSC Traces for Nifedipine–PVP Solid Dispersions
Arrows represent $T_g$.

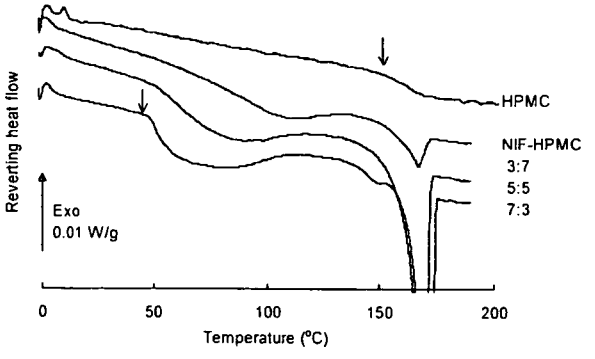


Fig. 6. DSC Traces for Nifedipine–HPMC Solid Dispersions
Arrows represent $T_g$.

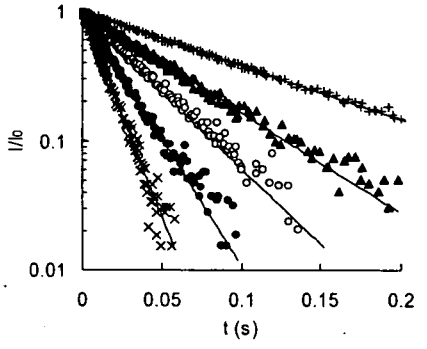


Fig. 7. $T_{1\rho}$ Decay Patterns for Nifedipine (+), HPMC (×), and Nifedipine–HPMC Solid Dispersions of 7 : 3 (▲), 5 : 5 (○), and 3 : 7 (●)

to confirm the phase structure of the solid dispersion, since the molecular mobility of PHPA may different from that of pure PHPA.

In contrast to PHPA, PVP and nifedipine in the solid dispersions (3 : 7, 5 : 5 and 7 : 3) were considered to be miscible from $T_{1\rho}$ relaxation and DSC measurements. Figure 4 shows typical $T_{1\rho}$ decay of the solid dispersions. All the solid dispersions studied exhibited mono-exponential $T_{1\rho}$ decay, whereas physical mixtures of amorphous nifedipine and PVP (3 : 7, 5 : 5 and 7 : 3) exhibited bi-exponential decay (data not shown). Figure 5 shows DSC traces for the nifedipine–PVP solid dispersions. A single glass transition was observed for all of the solid dispersions studied. These data indicate that nifedipine and PVP are miscible at the detection limit of NMR and DSC.

For nifedipine–HPMC solid dispersions, the miscibility of nifedipine and HPMC could not be assessed from $T_g$ measurements. As shown in Fig. 6, base line shift due to glass transition was not obvious for the nifedipine–HPMC solid dispersions (3 : 7 and 5 : 5). In contrast to DSC measurements, $T_{1\rho}$ relaxation measurements clearly indicated that nifedipine is miscible with HPMC in the solid dispersions. As shown in Fig. 7, all the nifedipine–HPMC solid dispersions studied showed mono-exponential $T_{1\rho}$ decay. In contrast to the solid dispersions, physical mixtures of amorphous nifedipine and HPMC (3 : 7, 5 : 5 and 7 : 3) exhibited bi-exponential decay (data not shown). These data indicate that NMR can detect miscibility of a drug and an excipient more sensitively than DSC.

Figure 8 shows the dissolution profile of nifedipine from

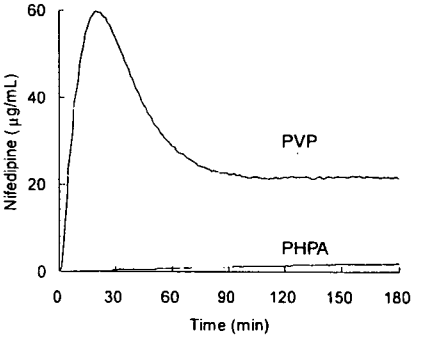


Fig. 8. Dissolution Profiles of Nifedipine from Solid Dispersions with PVP and PHPA

solid dispersions with PVP and PHPA. The nifedipine–PVP solid dispersion exhibited rapid dissolition of nifedipine with super-saturation. In contrast, only a minimal amount of nifedipine was dissolved from the nifedipine–PHPA solid dispersion.

In conclusion, $^1$H- NMR spin–lattice relaxation measurements were found to be useful for assessing the miscibility of a drug and excipients in solid dispersions, especially, when $T_g$ is not clearly detected by DSC. The lower miscibility of PHPA than that of PVP and HPMC with hydrophobic drugs is considered due to the more hydrophilic nature of PHPA.

**Acknowledgements** A part of this work was supported by a Grant-in-aid for Research on Publicly Essential Drugs and Medical Devices from The Japan Health Sciences Foundation.

**References**

1) Forster A., Hempenstall J., Tucker I., Rades T., *Int. J. Pharm.*, **226**, 147—161 (2001).
2) Lu Q., Zografi G., *Pharm. Res.*, **15**, 1202—1206 (1998).
3) Khougaz K., Clas S. D., *J. Pharm. Sci.*, **89**, 1325—1334 (2000).
4) Tong P., Zografi G., *J. Pharm. Sci.*, **90**, 1991—2004 (2001).
5) Vasanthavada M., Tong W. Q., Joshi Y., Kislalioglu M. S., *Pharm. Res.*, **21**, 1598—1606 (2004).
6) Shmeis R. A., Wang Z., Krill S. L., *Pharm. Res.*, **21**, 2025—2030 (2004).
7) Kaplan D. S., *J. Appl. Polym. Sci.*, **20**, 2615—2629 (1976).
8) Crowly K. J., Zografi G., *J. Pharm. Sci.*, **91**, 2150—2165 (2002).
9) Marsac P. J., Shamblin S. L., Taylor L. S., *Pharm. Res.*, **23**, 2417—2426 (2006).
10) Cheung M. K., *Polymer*, **41**, 1469—1474 (2000).
11) Asano A., Takegoshi K., "Solid State NMR of Polymers," Chap. 10, ed. by Ando I., Asakura T., Elsevier, Amsterdam, 1998, pp. 351—414.
12) Giammona G., Carlisi B., Plazzo S., *J. Polym. Sci. Polym. Chem. Ed.*, **25**, 2813—2818 (1987).
13) Kato Y., Watanabe F., *Yakugaku Zasshi*, **98**, 639—648 (1978).
14) Aso Y., Yoshioka S., Kojima S., *J. Pharm. Sci.*, **89**, 408—416 (2000).

日薬理誌（*Folia Pharmacol. Jpn.*）**131**，102～108（2008）

総説

# 抗体医薬の現状と展望

川西　徹

**要約**：抗体医薬は今現在最も活発に開発が行われている医薬品群の一つである．その背景としては，(1)異種タンパク質としての抗原性の壁を乗り越えるキメラ抗体あるいはヒト化抗体，ヒト抗体製造技術の完成，(2)ゲノム創薬による医薬品開発の標的となる数多くの疾患関連遺伝子および疾患関連タンパク質の解明，の2点があげられる．現在上市されている抗体医薬のほとんどは構造的にはIgGサブクラスであり，薬効からは主に抗腫瘍薬と免疫調節薬に分類されるが，今後は機能的に必要なコンポーネントに小型化した抗体や，細胞表面の受容体等と結合し細胞内情報伝達を引き起こすアゴニスト抗体，あるいは分子標的薬のコンポーネントとしての利用等，抗体医薬の利用は拡大してゆくことが予想される．しかしながら，これら次世代抗体医薬の開発にあたっては，薬理作用の解析，あるいは安全性予測という面で種差の壁があり，化学合成医薬品で通常用いられる齧歯類動物を主体とした非臨床試験による評価には限界がある．したがって，ヒト初回投与前の安全性予測においては，適切なインビトロ試験系の構築，適切な動物を用いたインビボ試験，さらにはトランスジェニック動物や相同タンパク質等を利用した試験等を組み合わせた試験による解析が必要であり，薬理学者の智恵と経験が必要とされる．

## 1.　はじめに

現在大学学部用の薬理学教科書を眺めてみると，タンパク質性高分子医薬品に関する記述は極めて限られたものであり，1000ページ弱の標準的教科書でみれば，占める割合は10ページにも満たないものがほとんどである．さらにその対象を抗体医薬に絞ると，抗腫瘍薬あるいは免疫調節薬の項の末尾に小さく扱われているだけで，多いものでも，あわせて2ページにも満たない．しかし眼を新薬開発の世界に転じると，今現在最も注目されている医薬品群の一つは抗体医薬であり，さらには従来の化学合成医薬品では治療が困難であった疾病治療の標準的治療薬の地位を確立しつつある抗体医薬も出現しており，近い将来，薬物治療の教科書の書き換えは必至の状況である．そこで，本稿では，このような抗体医薬開発ブームがおこった背景，代表的な抗体医薬を概説するとともに，今後現れることが予想される抗体医薬，さらには抗体医薬開発の今後の課題，および課題解決において薬理学の果たすべき役割について概説したい．

## 2.　今なぜ抗体医薬か？

21世紀初頭の現在，最も活発に開発が行われ，欧米を中心として新薬申請が活発な医薬品群の一つは抗体医薬である．振り返れば，抗体医薬開発ブームは1980年代に一度おこっている．その契機はKohler and Milsteinによるハイブリドーマを利用したモノクローナル抗体作製技術の確立にあった(1)．この技術によって，抗原に選択的に結合する抗体の効率的な生産が可能となり，癌治療への応用等が試みられた．しかしハイブリドーマモノクローナル抗体は，通常マウス由来の免疫グロブリンでありヒトに対しては異種タンパク質であるため抗原性が強く，ヒト体内で作られる中和抗体による作用の減弱，あるいはアナフィラキシーショックのため，医薬品としての利用は限定されたものとなった．

一方，現在の抗体医薬開発ブームは以下の2つを理由として生じたといえる．第一に組換えタンパク質作製技術，あるいはトランスジェニック動物作製技術等のバイオテクノロジーの飛躍的進歩により，キメラ抗体，ヒト化抗体等の遺伝子工学利用抗体の作製が可能

キーワード：抗体医薬，バイオテクノロジー応用医薬品，抗腫瘍薬，免疫調節薬
国立医薬品食品衛生研究所薬品部（〒158-8501 東京都世田谷区上用賀1-18-1）
e-mail: kawanish@nihs.go.jp　原稿受領日：2007年10月10日，依頼原稿
Title: Antibody drugs: the present status and perspectives.　Author: Toru Kawanishi

となったことである(2, 3)．これらの技術によって，従来のモノクローナル抗体が異種タンパク質であるゆえに生じた問題を回避できるようになった．

抗体医薬開発ブームが起こった第二の理由は，ゲノム創薬の本格化があげられる．ゲノム創薬は，生体の遺伝子あるいはタンパク質の構造，機能情報をもとに，医薬品シーズを発見，設計する医薬品開発手法であるが，今現在は疾病関連遺伝子あるいは疾病関連タンパク質の発見／特定，さらには疾病に至るメカニズムの解明は相次いでいるものの，これらの情報をもとに疾病治療用医薬品を効率的にデザインする手法の完成にまでは至っていない．その点で，疾病関連タンパク質に選択的に結合する抗体を生体の免疫系を利用して作製し，選別することにより最適の医薬品シーズを発見する手法は，様々な疾患関連タンパク質に対して共通に応用できる技術である．また，現在抗体医薬の開発に多くの企業が注力している理由としては，このような抗体医薬の開発の成功率の高さがあげられ，実際米国において第Ⅰ相臨床試験が実施されたもののうち上市に至った割合は低分子化合物では約5%であるのに対し，抗体医薬では約20%という報告もある(4)．

## 3. 遺伝子工学利用抗体の作製法

キメラ抗体とは遺伝子組換え技術を用いてマウスモノクローナル抗体の定常 constant（C）領域をヒト抗体のC領域に置き換えた抗体である．一方ヒト化抗体は抗体タンパク質の三次元構造をもとに，抗原に結合する相補性決定領域 complementarity determining region（CDR）の1から3を残して，それ以外の部分である抗体のフレーム領域 frame region（FR）を全てヒト抗体に置き換えたものである（図1）．以下に，マウスハイブリドーマ細胞から遺伝子組換え法によるキメラ抗体，ヒト化抗体の作製法を紹介する．

キメラ抗体作成の第一ステップは，マウス抗体産生ハイブリドーマからのマウス抗体をコードする遺伝子のクローニングである．通常ハイブリドーマ細胞よりRNAを抽出し，cDNAを作製後，プラークハイブリダイゼーション法あるいはPCR法により抗体遺伝子をクローニングする方法，あるいはRNAより直接PCR法により抗体遺伝子をクローニングする方法が用いられている．次にクローニングしたマウス抗体の可変（V）領域遺伝子にヒトのC領域遺伝子を連結し，適当な発現ベクターに挿入して培養細胞で生産する．また，抗体産生ハイブリドーマのマウス抗体C領域をヒト抗体C領域に組み換える相同組換え法やトランスジェニックマウスによっても作成される．

ヒト化抗体遺伝子の作製はさらに複雑なステップである．第一ステップではクローニングしたマウス抗体V領域における抗原との結合に寄与するCDR配列とヒト抗体V領域におけるアイソタイプ固有のアミノ酸配列をもつフレームワーク領域（FR）から成るV領域をコードする遺伝子を構築する．これにヒトのC領域遺伝子を連結し，構築された抗体 heavy（H）鎖および light（L）鎖遺伝子が挿入された発現ベクターを製造用動物細胞に導入し，遺伝子組換え抗体を発現する．製造細胞としては，チャイニーズハムスター卵巣由来のCHO細胞，マウスミエローマ由来のNS0細胞およびSP2/0細胞等が用いられることが多い(5)．

このようにヒト化抗体は高度な遺伝子組換え技術を利用して製造されるが，CDR配列部分はマウス由来である．そこですべてヒト由来の完全ヒト抗体の作成法が開発された．主な方法としては2種類あり，一つはファージディスプレイ法，一つはヒト抗体作製用トランスジェニックマウス法である．前者のファージディスプレイ法は大腸菌ウイルスの一つであるM13やT7などの繊維状ファージのコートタンパク質（g3p

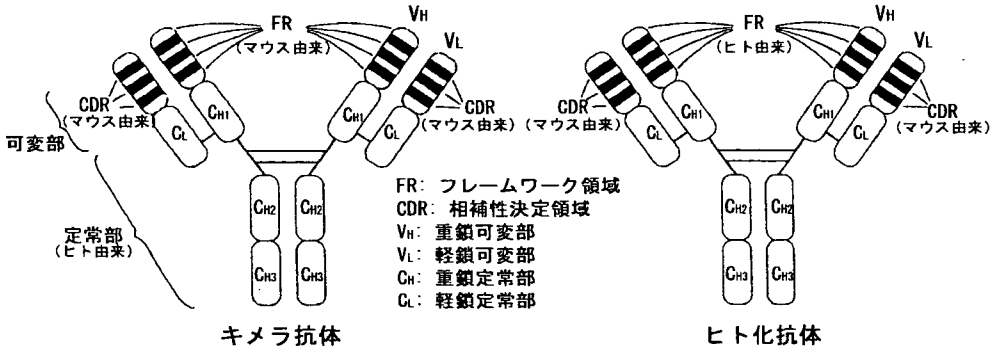


図1　キメラ抗体およびヒト化抗体の構造

表1 日米欧における既承認抗体医薬一覧[1)]

| 名称 | 商品名 | 種類 | 標的 | 主な適応疾患 | 承認をうけた年度 米国 | 欧州 | 日本 | 抗体生成頻度[2)] |
|---|---|---|---|---|---|---|---|---|
| 抗腫瘍薬 | | | | | | | | |
| Rituximab | Rituxan, MabThera | キメラ抗 IgG1κ | CD20 | B細胞性非ホジキンリンパ腫 | 1997 | 1998 | 2001 | <1% |
| Trastuzumab | Herceptin | ヒト化抗体 IgG1κ | HER2 | 転移性乳ガン | 1998 | 2000 | 2001 | 0.1% |
| Denileukin Diftitox | Ontak | 融合タンパク質 IL2 + Diphtheria toxin | IL2R | 皮膚T細胞リンパ腫 | 1999 | NA[3)] | NA | 8% |
| Gemtuzumab ozogamicin | Mylotarg | ヒト化抗体 IgG4κ（カリケアマイシン結合） | CD33 | 急性骨髄性白血球 | 2000 | NA | 2005 | |
| Alemtuzumab | Campath, MabCampath | ヒト化抗体 IgGaκ | CD52 | B細胞性慢性リンパ性白血病 | 2001 | 2001 | NA | <2% |
| Ibritumomab tiuxetan | Zevalin | マウス抗体 IgG1κ ($^{90}$Y標識) | CD20 | B細胞性非ホジキンリンパ腫 | 2002 | 2004 | NANA | |
| Iodine 131 Tositumomab | Bexxar | マウス抗体 IgG2aλ ($^{131}$I標識) | CD20 | 非ホジキンリンパ腫 | 2003 | NA | NA | |
| Cetuximab | Erbitux | キメラ抗体 IgG1κ | EGFR | 頭頸部癌，結腸・直腸癌 | 2004 | 2004 | NA | 5% |
| Bevacizumab | Avastin | ヒト化抗体 IgG1 | VEGF | 結腸・直腸癌 | 2004 | 2005 | 2007 | ND |
| Panitumumab | Vectibix | ヒト化抗体 IgG2κ | EGFR | 結腸・直腸癌 | 2006 | NA | NA | |
| 免疫調節薬 | | | | | | | | |
| Muromonab-CD3 | Orthoclone OKT3 | マウス抗体 IgG2a | CD3 | 腎移植後の急性拒絶反応 | 1986 | NA | 1991 | ~80% |
| Daclizumab | Zenapax | ヒト化抗体 IgG1κ | CD25 | 腎移植後の急性拒絶反応 | 1997 | 1999 | NA | |
| Basiliximab | Simulect | キメラ抗体 IgG1κ | CD25 | 腎移植後の急性拒絶反応 | 1998 | 1998 | 2002 | <2% |
| Infliximab | Remicade | キメラ抗体 IgG1κ | TNFα | 関節リウマチ | 1998 | 1999 | 2002 | 10-57% |
| Etanercept | Enbrel | 融合タンパク質 TNFαR + Fc | TNFα | 関節リウマチ関節リウマチ | 1998 | 2000 | 2005 | |
| Adalimumab | Humira | ヒト抗体 IgG1κ | TNFα | 関節リウマチ | 1998 | 2002 | 2003 | NA |
| Efalizumab | Raptiva | ヒト化抗体 IgG1κ | CD11 | 尋常性乾癬 | 2003 | 2004 | NA | |
| Omalizumab | Xolair | ヒト化抗体 IgG1κ | IgE | 喘息 | 2003 | 2003 | 2005 | NA |
| Alefacept | Amevive | 融合タンパク質 LFA3 + Fc | CD2 | 尋常性乾癬 | 2003 | NA | NA | |
| Natalizumab | Tysabri | ヒト化抗体 IgG4κ | α4integrin | 多発性硬化症 | 2004 | 2006 | NA | |
| Abatacept | Orencia | 融合タンパク質 CTLA4 + Fc | CD80/CD86 | 関節リウマチ | 2005 | NA | NA | |
| Tocilizumab | Actemra | ヒト化抗体 IgG1κ | IL6R | キャッスルマン病 | NA | NA | 2005 | |
| Eculizumab | Soliris | ヒト化抗体 IgG2/4κ | C5a | 発作性夜間血色素尿症 | 2007 | 2007 | NA | |
| その他 | | | | | | | | |
| Abciximab | ReoPro | キメラ抗体 IgG1（Fab） | GPIIb/IIIa | 心筋虚血 | 1994 | NA | NA | 7-19% |
| Palivizumab | Synagis | ヒト化抗体 IgG1κ | RSVFProtein | RSウィルス感染 | 1998 | 1999 | 2002 | <1% |
| Ranibizumab | Lucentis | ヒト化抗体 IgG1κ（48Kフラグメント） | VEGF-A | 加齢黄斑変性 | 2006 | 2007 | NA | |

1）文献9より改変，2）文献10中の値，3）NA：未承認

やg10pなど）のN末端側にファージの感染性を失わないよう外来遺伝子を融合タンパク質として発現させるシステムである．一度に$10^8$種類以上ともいわれる多種類の分子種を呈示したライブラリーを構築でき，また粒子ごとに目的の機能や性質をもった分子種を選択できる．この技術を用いて外来遺伝子として抗体の結合部位である2つのポリペプチド鎖VHとVLを短いリンカーで直列につないだ単鎖Fv single-chain Fv（scFv）をファージにディスプレイさせたものが抗体ファージライブラリーである．そしてファージライブラリーから特異的抗体ファージをスクリーニングする．これを最終的にファージから切り離したものがファージディスプレイ抗体である(6, 7)．

完全ヒトモノクローナル抗体取得のもう一つの方法は，ヒト抗体を産生するトランスジェニック動物の利用である．内因性Igをノックアウトしたマウスに機能的なヒトのIg遺伝子を導入すれば，マウス抗体の代わりに多様な抗原結合能を持つヒト抗体が産生されると考えられる．さらにこのマウスを免疫すればヒトモノクローナル抗体を従来のハイブリドーマ法で得ることが可能である．既にKMマウス，KWマウス，HACマウス等のヒト抗体産生用マウスが開発され，完全ヒト抗体の製造に利用されている(8)．

## 4. 遺伝子工学利用抗体医薬の利点

2. においてキメラ抗体，ヒト化抗体，ヒト抗体の利点として，異種タンパク質ゆえの抗原性の克服について言及したが，表1に日米欧で認可をうけている抗体医薬に対するヒトでの抗体の検出頻度を記した．この数字から明らかなように，ハイブリドーマ抗体医薬では，極めて高い頻度の抗体医薬に対する抗体の出現が報告されている．一方，キメラ抗体においてはフレームワークを含む可変領域が抗原性を残しているため，抗体によって高い抗体生成が報告されている製品はあるものの，ハイブリドーマ抗体に比べれば全般的に抗体生成頻度は低い．ヒト化抗体は，理論的には抗原性を示す部位はマウス由来のCDR配列のみであり，比較的低い数字が報告されている(10)．

このような中和抗体の生成とも関連することであるが，ハイブリドーマ抗体については，ヒト抗体と比較してヒト血中半減期が極めて短いことが指摘されてきた（ヒト抗体：23日，ハイブリドーマ抗体：1-3日）．また，組換えキメラ抗体，ヒト化抗体においては，ハイブリドーマ抗体に比べると，一般に血中半減期が長いことが報告されている．このメカニズムが最近になって明らかになってきた．即ち，母親から胎児に液性免疫を伝える機構を担うIgG胎児性Fc受容体(FcRn)は，成長後も免疫グロブリンの体内循環を担うことにより血中半減期の延長に役だっていること，さらには疾病治療用抗体医薬の血中半減期の改善に，IgGのFc領域とFcRnとの相互作用が利用できることが明らかにされている(11, 12)．

## 5. 既に上市されている主な抗体医薬

現在までに日米欧で認可された抗体医薬を表1にまとめた．対象疾患は様々であるが，大別すると主に抗腫瘍薬，および免疫調節薬に分類される．抗腫瘍薬としてはリツキシマブ，トラスツズマブ，ゲムツズマブオゾガマイシン，ベバシズマブ等は，現在標準的治療に使用される医薬品としての評価を得るまでになっている．また免疫調節薬のなかで，インフリキシマブはメトトレキセートの併用薬として関節リウマチの治療に使用されることが多い．さらにヒト型遺伝子組換え可溶性TNFα受容体-Fc融合タンパク質のエタネルセプトは，IgGではなく抗体のFc領域を利用した人工タンパク質であるが，メトトレキセートとの併用の必要のない関節リウマチ治療薬である．加えて日本発であるヒト化抗IL-6受容体抗体トシリズマブ（中外製薬と大阪大学の共同開発）は，キャッスルマン病治療薬として認可されたが，関節リウマチへの適用拡大を目指した試験で好成績を得たとされている．

このように，多くの抗体医薬が疾病治療に有効であることが示され，新薬として脚光をあびている．

## 6. 今後開発が予想される次世代抗体医薬

以上のように，抗体医薬は欧米を中心に既に数多くの製品が承認されているが，既承認抗体医薬は融合タンパク質型以外の製品では，いずれも構造的にはIgGのサブクラスに属し，機能的にも構造的にも分離可能な2つのモジュール：1）抗体認識部位であるV領域：2）抗体が抗原に結合した後のCDC（Complement Dependent Cytotoxicity 補体依存性細胞障害：抗体が細胞膜表面上の抗原決定基に特異的に結合して，補体の介助のもとで，その細胞に傷害を与えること）活性あるいはADCC（Antibody Dependent Cell-mediated Cytotoxicity 抗体依存性細胞傷害：IgGクラス抗体のFc領域がT細胞，NK細胞，好中球，マクロファージ上のFc受容体を介して，これらエフェクター細胞を活性化し，抗体の可変領域が結合した細胞を殺すこと）活性等の反応を惹起するエフェクター機能を担うFc領域から構成されている．しかしこのようなIgG抗体医薬の分子量は10万をこえる巨大分子であるた

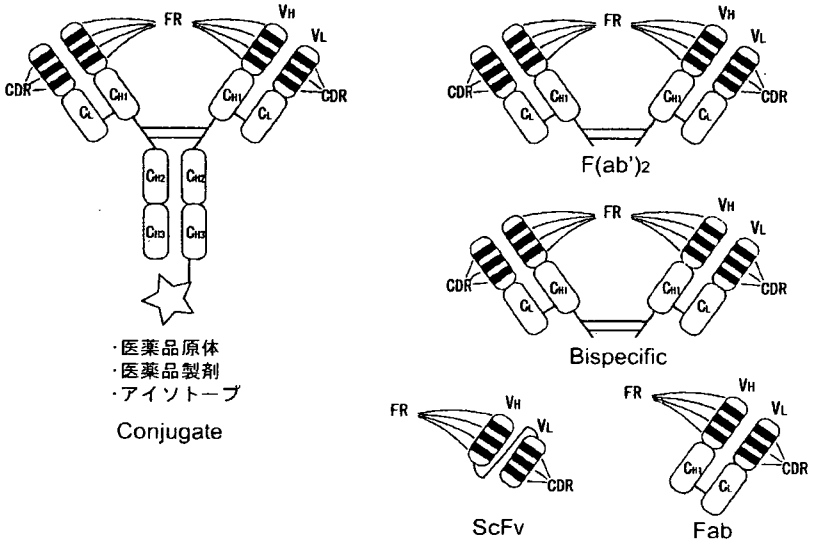


**図2 今後出現すると思われる次世代抗体医薬**
(文献13より改変)

め，血中から組織への移行はきわめて遅い．その解決策としてファージディスプレイなどの方法を用いたScFvタイプ，あるいはFabタイプ，$F(ab')_2$タイプ等，サイズを小さくし，生体内移行性を増大する抗体医薬の検討が行われている（図2）．さらには，異なる抗原特異性を有する抗体に由来するFabフラグメントをつなぎ，2つの特異性bispecificを有する$F(ab')_2$タイプの医薬品としての利用も試みられている．一方このような低分子化抗体は，既存の化学合成医薬品原体，あるいは医薬品製剤に結合させることにより，これら医薬品に標的性を付与させることが可能となるので，今後分子標的薬開発のコンポーネントとしての利用も活発化することが予想される．

以上のような抗体のアミノ酸配列部分の改変以外に，糖鎖改変抗体の作製も試みられている．既承認の抗体医薬のほとんどはIgG型であり，Fc部分のCH2領域にアスパラギン結合型のコンプレックス型糖鎖を持つ糖タンパク質である．抗体の糖鎖は共通のコア部分に，修飾が異なる30種類以上のオリゴ糖の末端がついた混合物であるが，この糖鎖の付け根に付いているフコースがなくなるとADCC活性が動物レベルで100倍上昇する．したがって，抗体のFc領域に結合している糖鎖からフコース残基を除去すると，高いADCC活性が誘導される(14, 15)．

以上のような，構造的に新しいタイプの抗体医薬とともに，作用機構の上でも新しいタイプの抗体医薬の創製が活発化するものと考えられる．即ち，従来の抗体医薬の多くは疾病関連タンパク質への親和性を利用し，(1)これらタンパク質を中和，(2)酵素や受容体等の反応をブロック，(3)細胞膜の標的タンパク質に結合しFc領域のエフェクター機能による細胞傷害等によって薬理作用を発現する．しかし次世代の抗体医薬としては，細胞表面受容体等（例えばトロンビン受容体，エリスロポエチン受容体，成長ホルモン受容体，FAS，CD20，CD28）に結合し，アゴニストとして細胞内情報伝達を引き起こすことを目指したアゴニスト抗体の開発も精力的に行われている．

## 7. 次世代抗体医薬の薬理作用の解析および安全性評価

以上のように，抗体医薬開発は広汎かつ活発に行われているが，昨年3月このような抗体医薬の安全性評価法の信頼を揺るがす臨床試験事故が起こった．問題となった医薬品候補化合物はTリンパ球表面のCD28に結合するヒト化モノクローナル抗体TGN1412で，ドイツのTeGenero社によって開発されていた抗CD28アゴニスト抗体（スーパーアゴニスト）であった．従来のモノクローナル抗体では，単独でT細胞を活性化できないが，このスーパーアゴニストは結合部位の違いから単独でT細胞を活性化させ，T細胞の増殖およびサイトカイン産生を誘導することができるとされ，B細胞慢性リンパ球白血病等の血液系の悪性腫瘍や関節リウマチ等の慢性炎症性疾患の治療薬として開発が進められていた(16, 17)．初回臨床試験は0.1

mg/kg の静脈投与で実施されたが，被験者 6 名全員に重度のサイトカイン放出症候群が生じ，多臓器不全に陥った．症状は極めて重篤であったものの，救命処置により幸い死亡には至らなかった(18)．この事故が臨床試験の専門家を混乱に陥れたのは，この薬は欧州規制当局 EMEA によりオーファン薬として指定をうけ，治験申請についても当然のことながら規制当局からの承認をうけていたことである．

事故の原因分析は，英国および欧州規制当局によって詳細に実施されている(19, 20)．まずこの治験に使われたロットについての品質面の詳細な分析の結果，不純物等の品質の問題による事故でないことが明らかにされた．そこで，検討はヒト初回投与試験における投与方法と用量の妥当性を中心に行われた．まず投与方法についてであるが，カニクイザルでの実験が 1 時間をかけた点滴注射で行われたのに対して，ヒト初回投与試験では短時間(1-5 分）の静注を行った点は，サイトカイン放出症候群を招いた原因として充分考えられるポイントである．一方初回臨床試験の投与用量であるが，カニクイザルでの 28 日間反復投与試験結果で，5 mg/kg および 50 mg/kg 投与によりリンパ球の活性化，それを反映した IL-5，IL-6 の上昇がみられたものの，これらの作用は薬理作用と考え，それ以外には特段の有害作用はみられなかったと判断，無毒性量 NOAEL を 50 mg/kg とし，この数字をもとに安全率を 500 倍とって決定したものであり(21)，従来の評価法の基準からすると必ずしも間違いとはいえない．しかし，英国 National Institute of Biological Standards and Control（NIBSC）の報告では，TGN1412 の作用のインビトロ検出系を新たに構築，その解析結果によると，カニクイザルのリンパ球では TGN1412 による細胞増殖やサイトカイン産生は検出されないが，ヒトリンパ球ではどちらも検出できアゴニスト作用が確認できること，しかもその濃度作用曲線はベル型を示し，至適濃度は 2-10 μg/ml であることを見いだしている(22)．この結果は，カニクイザルの実験ではヒトの作用の予測が困難な場合があることを示している．

バイオテクノロジー応用タンパク質性医薬品の安全性評価については，(1)従来の医薬品のほとんどは物質的にも天然のヒトタンパク質に限りなく近いことを目標に設計されている，(2)したがって生理的条件と同様な暴露条件なら，作用は予測可能である，(3)齧歯類動物を中心とした非臨床試験は，種差の壁により薬理作用および毒性の解析は困難な場合が少なくない，(4)試験動物にとって被験物質は異種タンパク質であり，中和抗体の生成等によって正確な作用プロファイルの解析は困難である．したがって，これら医薬品の非臨床安全性試験ガイドライン(23）では，動物を用いる非臨床試験の有用性は化学合成医薬品の場合に比べて限られるとされ，また，ヒト型標的タンパク質を発現させたトランスジェニック動物，あるいは相同タンパク質による検討を推奨している．このガイドラインが運用され，既に 7 年が経過しているが，トランスジェニック動物あるいは相同タンパク質は，未だ推奨の段階に終わっているのが実状である．一方，アゴニスト抗体は天然の生理活性物質とは異なる薬理作用を示すことが期待されて作製されるタンパク質であり，生物学的な実験なしに作用の予測は困難である．また低分子抗体はヒト抗体と同様の特異性を有しているとしても，ヒト抗体では分布しえない体内部位に分布し作用する．したがって，今後これらの新しいタイプの抗体医薬をヒトに投与するにあたっての作用の解析は，適切なインビトロ系の構築，適切な種の動物を用いたインビボ解析，さらに可能な場合は相同タンパク質あるいはトランスジェニック動物等の利用によって，作用機構の解析，濃度作用相関あるいは用量作用相関の解析を行うことが必要である．EU ではすでに，これらハイリスク薬のヒト初回臨床試験において考慮すべき要件をまとめたガイドラインを作成しており，投与量を決定する場合は，最小予測生物学的影響量 Minimal Anticipate Biological Effect Level（MABEL）に基づくこと等の推奨を盛り込んでいる(24)．

## 8. おわりに

抗体医薬の開発は活発に行われており，近い将来薬理学の教科書にも大幅に取り入れる必要が生じるであろう．さらに今後構造面からも作用機構からも新しいタイプの抗体医薬開発が活発化することが予想される．このような次世代抗体医薬の開発においては薬理作用の解析，および安全性予測のためには，インビボ，インビトロ実験系を駆使した薬理作用の解析が重要であり，その解析には薬理学者の智恵と経験が必要とされる．

**謝辞**：本総説に関わる研究の一部は，厚生労働省科学研究費補助金医薬品・医療機器レギュラトリーサイエンス総合研究事業に対する助成金によるものである．ここに謝意を表する．

## 文　献


1) Kohler G, et al. Nature.1975:256:495-497.
2) Morrison SL, et al. Chimeric immunoglobulin genes:Immunoglobulin genes. Academic Press;1989.p.260-278.
3) Roguska MA, et al. Proc Natl Acad Sci USA. 1994;9:969-973.
4) Chapman K, et al.Nature Rev. 2007;6:120-126.
5) Chu L, et al. Curr Opin Biotechnol. 2001;12:180-187.
6) Winter G, et al. Ann Rev Immunol. 1994;12:433-455.
7) Burton DR, et al. Adv Immunol. 1994;57:191-280.
8) 石田　功．実験医学．2002;20:846-851.
9) 山口照英，他．谷本学校毒性質問箱．2007;10:(印刷中)
10) Koren E, et al. Curr Pharm Biotechnol. 2002;3:349-360.
11) Lobo ED, et al. J Pharm Sci. 2004;93:2645-2668.
12) Roopenian DC, et al. Nature Rev. 2007;7:715-725.
13) VanDijk MA, et al. Monoclonal Antibody-Based Pharmaceuticals: Pharmaceutical Biotechnology 2nd Ed. Taylor & Francis;2002. p.283-299.
14) Shinkawa T, et al. J Biol Chem. 2002;278:3466-3473.
15) Shields RL, et al. J Biol Chem. 2002;277:26733-26740.
16) Beyersdorf N, et al. Ann Rheum Dis. 2005;64 Suppl 4：iv91-95.
17) Margulies DH. J Exp Med. 2003;197:949-953.
18) Suntharalingam G, et al. N Engl J Med. 2006;355:1018-1028.
19) Early stage clinical trial taskforce; Joint ABPI/BIA report. [cited; Available from:http://www.abpi.org. uk/information/pdfs/BIAABPI_taskforce2.pdf
20) Expert group on phase one clinical trials: Final report.[cited; Available from: http://www.dh.gov. uk/en/Publicationsandstatistics/Publications/PublicationsPolicyAndGuidance/DH_063117
21) Kenter MJ, et al. Lancet. 2006;368:1387-1391.
22) Stebbings R, et al. J Immunol. 2007;179:3325-3331.
23) バイオテクノロジー応用医薬品の非臨床における安全性評価. [cited; Available from:http://www.pmda.go. jp/ich/s/s6_00_2_22.pdf]
24) Guideline on strategies to identify and mitigate risks for first-in-human clinical trials with investigational medicinal products. [cited;Available from:http://www.emea.europa.eu/pdfs/human/swp/2836707enfin.pdf]


### 著者プロフィール


川西　徹（かわにし　とおる）

国立医薬品食品衛生研究所 薬品部 部長，博士（薬学）．◇1977年東京大学大学院薬学系研究科修士課程修了，同年国立衛生試験所（現国立医薬品食品衛生研究所）安全性生物試験研究センター薬理部研究員（この間，カリフォルニア大学バークレー校，ノースカロライナ大学チャペルヒル校で博士研究員），同安全性生物試験研究センター病理部室長，同生物薬品部室長，同生物薬品部長を経て2006年4月より現職．◇専門領域：医薬品評価科学（一般薬理，薬物代謝，化学物質リスクアセスメント，細胞毒性評価法開発，顕微鏡画像解析法開発，細胞内生化学現象の可視化技術開発，生物薬品特性解析法開発，製剤評価法開発）

J Pharmacol Sci 103, 241 – 246 (2007)

*Journal of Pharmacological Sciences*


*Full Paper*

# Involvement of the $Na^+/Ca^{2+}$ Exchanger in Ouabain-Induced Inotropy and Arrhythmogenesis in Guinea-Pig Myocardium as Revealed by SEA0400

Hikaru Tanaka[1,*], Hideaki Shimada[1], Iyuki Namekata[1], Toru Kawanishi[2], Naoko Iida-Tanaka[1,3], and Koki Shigenobu[1]

[1]*Department of Pharmacology, Toho University Faculty of Pharmaceutical Sciences, Funabashi, Chiba 274-8510, Japan*
[2]*Division of Biological Chemistry and Biologicals, National Institute of Health Sciences, Tokyo 158-8501, Japan*
[3]*Department of Food Science, Otsuma Woman's University, Chiyoda-ku, Tokyo 102-8357, Japan*

*Received August 10, 2006; Accepted December 19, 2006*

**Abstract.** Involvement of the $Na^+/Ca^{2+}$ exchanger in ouabain-induced inotropy and arrhythmogenesis was examined with a specific inhibitor, SEA0400. In right ventricular papillary muscle isolated from guinea-pig ventricle, 1 $\mu$M SEA0400, which specifically inhibits the $Na^+/Ca^{2+}$ exchanger by 80%, reduced the ouabain (1 $\mu$M)-induced positive inotropy by 40%, but had no effect on the inotropy induced by 100 $\mu$M isobutyl methylxantine. SEA0400 significantly inhibited the contracture induced by low $Na^+$ solution. In HEK293 cells expressing the $Na^+/Ca^{2+}$ exchanger, 1 $\mu$M ouabain induced an increase in intracellular $Ca^{2+}$, which was inhibited by SEA0400. The arrhythmic contractions induced by 3 $\mu$M ouabain were significantly reduced by SEA0400. These results provide pharmacological evidence that the $Na^+/Ca^{2+}$ exchanger is involved in ouabain-induced inotropy and arrhythmogenesis.

***Keywords***: ouabain, $Na^+/Ca^{2+}$ exchanger, SEA0400, inotropy, arrhythmia

## Introduction

The $Na^+/Ca^{2+}$ exchanger (NCX) is involved in the physiological and pathophysiological regulation of $Ca^{2+}$ concentration in the myocardium. It is considered to function both in the forward ($Ca^{2+}$ extrusion) and reverse ($Ca^{2+}$ influx) modes. The major role of myocardial NCX is to extrude $Ca^{2+}$ from the cell through the forward mode and produce relaxation. Contribution of reverse mode NCX to $Ca^{2+}$ entry during the early phase of normal myocardial contraction has also been postulated. The mode of NCX action possibly changes during the contractile cycle and the balance may vary with factors such as the animal species, developmental stage and the condition of the myocardium (1, 2). NCX activity is closely related to intracellular $Ca^{2+}$ handling and is involved in normal and abnormal myocardial pacemaking (3).

*Corresponding author. htanaka@phar.toho-u.ac.jp
Published online in J-STAGE
doi: 10.1254/jphs.FP0060911

NCX has also been considered to be involved in cardiac glycoside-induced positive inotropy (4). Cardiac glycosides, which inhibit the sodium-potassium pump, would increase intracellular $Na^+$ concentration, which in turn shifts the mode of NCX towards the reverse mode, and produce positive inotropy through an increase in intracellular $Ca^{2+}$ concentration. Extensive evidence has been presented for this view including studies with fetal myocardial tubes from NCX knockout mouse (5). However, pharmacological assessment of the role of NCX in cardiac glycoside-induced inotropy and arrhythmogenesis has been limited because of the lack of an NCX inhibitor with sufficient specificity.

SEA0400 {2-[4-[(2,5-difluorophenyl)methoxy]phenoxy]-5-ethoxyaniline} is a potent and selective inhibitor of NCX in cultured rat neurons, astrocytes, microglia, and myocytes and dog sarcolemmal vesicles with negligible affinities towards other transporters, ion channels, and receptors (6 – 9). We have previously examined the effects of SEA0400 on the myocardial NCX current using voltage clamped guinea-pig ventricular myocytes (7) and found that SEA0400 concentra-

tion-dependently inhibits the NCX current with $IC_{50}$ values of 40 and 32 nM for the forward and reverse modes, respectively. This was confirmed with NCX1 expressed in HEK93 cells (10). SEA0400 (1 $\mu$M), which inhibited NCX current by more than 80%, had no effect on the $Na^+$ current, L-type $Ca^{2+}$ current, delayed rectifier $K^+$ current, and inwardly rectifying $K^+$ current (7) and the $Ca^{2+}$ sensitivity of contractile proteins (11). KB-R7943, which has been used as an inhibitor of NCX, was revealed to have virtually no selectivity for these ion channels and transporters (7). Thus, SEA0400 can become the first specific pharmacological tool to study the role of NCX and was shown to be useful in studies on myocardial excitation-contraction mechanisms, regulation by autonomic transmitters, and ischemia-reperfusion injury (6, 11 – 17).

Concerning the action of cardiac glycosides, inhibition by SEA0400 of digitalis-induced arrhythmias in canine models was reported (18), but the mechanisms of cardiac glycoside-induced inotropy and arrhythmogenesis has not been examined in the isolated working myocardium with this selective inhibitor. The present study was performed to obtain pharmacological evidence for the involvement of NCX in cardiac glycoside-induced inotropy and arrhythmogenesis.

## Materials and Methods

*Measurement of contractile force and contracture in papillary muscle preparations*

Isolated papillary muscle preparations were made, and contractile force was measured with standard techniques as described (19). Contracture induced by a low sodium solution was used as an index of reverse-mode NCX activity as described earlier (20) with a slightly modified protocol. The initial extracellular solution was of the following composition and gassed with 95% $O_2$ – 5% $CO_2$: 113.1 mM NaCl, 4.6 mM KCl, 2.45 mM $CaCl_2$, 1.2 mM $MgCl_2$, 21.9 mM $NaHCO_3$, and 10 mM glucose (pH 7.4). After the contractile force reached the steady state, stimulation was ceased. The preparation was incubated for 30 min with or without 1 $\mu$M SEA0400, and thereafter the solution was changed to a low-sodium solution. The low-sodium solution was prepared with the equimolar substitution of tetramethyl-ammonium chloride for NaCl in a modified Krebs solution, so that the final $Na^+$ concentration was 21.9 mM. This solution also contained 10 $\mu$M monensin, 20 mM caffeine, and 4.9 mM $CaCl_2$. The amplitude of low-sodium contracture was expressed as the percentage of steady-state developed tension. SEA0400 (1 $\mu$M) was applied from 30 min before the low-sodium perfusion and kept in the low-sodium solution continuously.

*Preparation of HEK293 cells expressing NCX and measurement of cytoplasmic $Ca^{2+}$ concentration*

HEK293 cells stablly expressing bovine NCX1 were obtained in our previous study (10). Cytoplasmic $Ca^{2+}$ was monitored with the fluorescent probe fura 2. The cells were loaded with 5 $\mu$M fura 2/AM for 30 min at 37°C. They were excited at 340 and 380 nm, and emission (>500 nm) was separated with a dichroic mirror. Data acquisition and analysis were performed with the aquacosmos system (Hamamatsu Photonics, Hamamatsu). Calibration was performed *in situ* as in our previous study (17).

*Drugs and chemicals*

SEA0400 was provided by Taisho Pharmaceutical Company, Ltd. (Saitama). The drug was dissolved in dimethyl sulfoxide (final concentration of 0.01%). Fura 2 was obtained from Dojin (Kumamoto). All other chemicals were of the highest commercially available quality.

*Data and statistics*

Statistical significance between means was evaluated by Student's $t$-test or by the $\chi^2$-test, and a $P$ value less than 0.05 was considered significant.

## Results

*Effect of SEA0400 on contracture induced by low-sodium solution*

The inhibitory activity of SEA0400 on reverse mode NCX was confirmed in myocardial tissue preparations (Fig. 1). Treatment of ventricular tissue preparations with a low $Na^+$ extracellular solution resulted in muscle contracture. SEA0400 (1 $\mu$M) significantly decreased the contracture; the magnitude of the contracture in the absence and presence of SEA0400 at 30 min was 134.7 ± 34.2% and 43.4 ± 18.4% (n = 10), respectively, of the initial contractile force.

*Effect of SEA0400 on ouabain-induced inotropy*

Effect of SEA0400 on ouabain-induced inotropy was examined in papillary muscles isolated from guinea-pig right ventricle (Fig. 2). SEA0400 showed no significant inotropic effects; the contractile force after the application of 1 $\mu$M SEA0400 was 105.3 ± 10.0% (n = 6) of that before application. Ouabain (1 $\mu$M) induced a gradual increase in contractile force; the contractile force at 30 min after addition of ouabain was 473.5 ± 44.7% (n = 6) of that before addition. SEA0400 (1 $\mu$M) significantly reduced the ouabain-induced

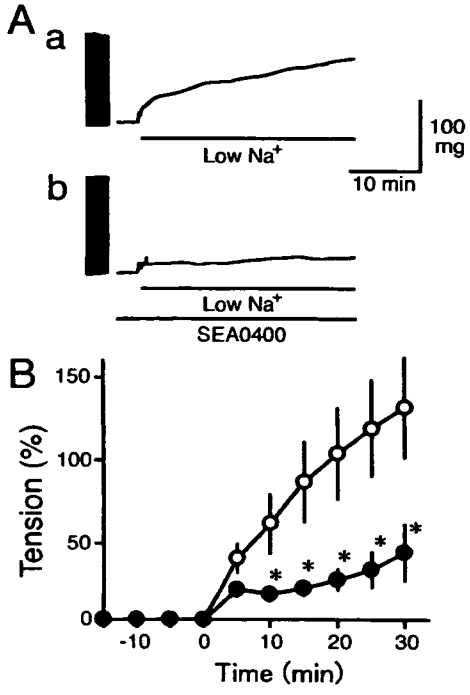


**Fig. 1.** Effect of SEA0400 on low $Na^+$-induced contracture in papillary muscles. A: Typical records of contracture induced by low $Na^+$ solution in the absence (a) and presence (b) of 1 $\mu$M SEA0400. B: Summarized results for the contracture. Increase in basal tension was expressed as a percentage of the stimulation-evoked contractile force in the same preparation. Each point with vertical bars represents the mean ± S.E.M. of 10 experiments. Asterisks indicate significant difference ($P$<0.05) from the corresponding values in the absence (open circles) of SEA0400.

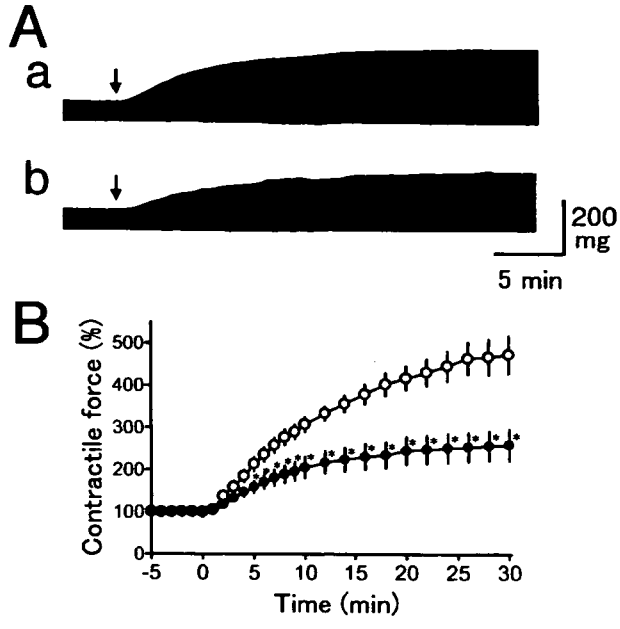


**Fig. 2.** Effects of SEA0400 on ouabain-induced inotropy. A: Typical records showing the effects of 1 $\mu$M ouabain in the absence (a) and presence (b) of 1 $\mu$M SEA0400. Arrows indicate the addition of 1 $\mu$M ouabain. B: Summarized results in the absence (open circles) and presence (closed circles) of SEA0400. Contractile force after the addition of 1 $\mu$M ouabain was expressed as a percentage of the contractile force before the addition. Each point with vertical bar represents the mean ± S.E.M. of 6 experiments. Asterisks indicate significant difference ($P$<0.05) from the corresponding values in the absence of SEA0400.

positive inotropy; in the presence of 0.3, 1, and 10 $\mu$M SEA0400, the contractile force at 30 min after addition of ouabain was 394.1 ± 32.9% (n = 6), 259.3 ± 37.1% (n = 6), and 279.8 ± 32% (n = 7) of that before addition, respectively.

*Effect of SEA0400 on IBMX-induced inotropy*

Effect of SEA0400 on IBMX-induced inotropy was examined in the papillary muscles (Fig. 3). IBMX (100 $\mu$M) induced a rapid increase in contractile force; the contractile force at 5 min after addition of ouabain was 281.7 ± 19.4% (n = 6) of that before addition. SEA0400 (1 $\mu$M) did not affect the IBMX-induced positive inotropy; in the presence of SEA0400, the contractile force at 30 min after addition of IBMX was 280.7 ± 19.4% (n = 6) of that before addition.

*Dependence of ouabain effects on NCX*

Dependence of ouabain effects on NCX was examined with HEK293 cells (Fig. 4). Treatment of HEK293cells expressing the NCX1 protein with low $Na^+$ solution resulted in an increase in cytoplasmic $Ca^{2+}$ concentration that reflects reverse mode NCX activity. In such cells, ouabain induced a gradual increase in cytoplasmic $Ca^{2+}$ concentration. The cytoplasmic $Ca^{2+}$ concentration before and 20 min after the addition of 10 $\mu$M ouabain was 46.4 ± 4.5 and 621.5 ± 57.3 nM (n = 17), respectively. This ouabain-induced increase in cytoplasmic $Ca^{2+}$ concentration was completely inhibited by SEA0400. In the presence of 1 $\mu$M SEA0400, the cytoplasmic $Ca^{2+}$ concentration before and 20 min after the addition of 10 $\mu$M ouabain was 58.8 ± 8.0 and 37.9 ± 7.8 nM (n = 17), In wild type HEK293 cells, the lack of functional NCX activity was confirmed by lack of increase in cytoplasmic $Ca^{2+}$ concentration by low $Na^+$ solution. Ouabain induced no significant increase in cytoplasmic $Ca^{2+}$ concentration in wild type HEK293 cells, indicating the dependence of ouabain action on NCX function. In wild type HEK293 cells, the cytoplasmic $Ca^{2+}$ concentration before and 20 min after the addition of 10 $\mu$M ouabain was 45.2 ± 8.4 and 54.7 ± 8.6 nM (n = 24) (not shown in the figure).

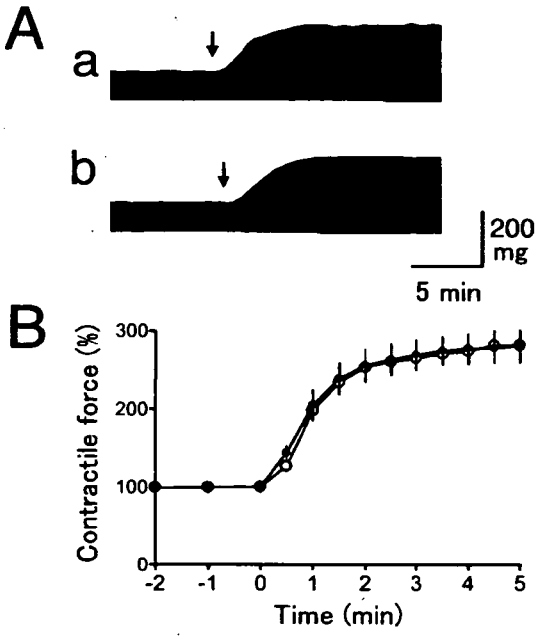


**Fig. 3.** Effects of SEA0400 on IBMX-induced inotropy. A: Typical records showing the effects of 100 $\mu$M IBMX in the absence (a) and presence (b) of 1 $\mu$M SEA0400. Arrows indicate the addition of 100 $\mu$M IBMX. B: Summarized results in the absence (open circles) and presence (closed circles) of SEA0400. Contractile force after the addition of 100 $\mu$M IBMX was expressed as a percentage of the contractile force before the addition. Each point with vertical bar represents the mean ± S.E.M. of 6 experiments.

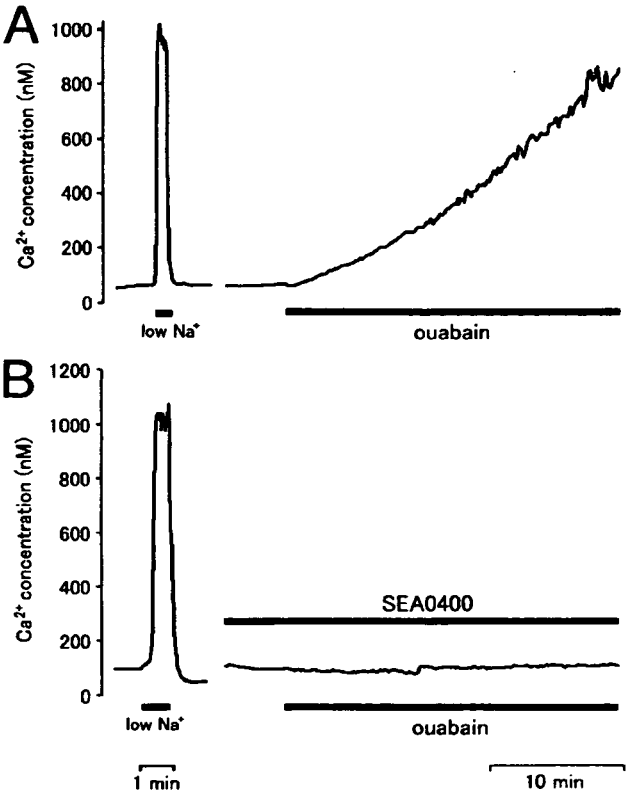


**Fig. 4.** Effect of ouabain on intracellular $Ca^{2+}$ in HEK293 cells expressing NCX loaded with fura-2. Typical records of changes in intracellular $Ca^{2+}$ concentration in response to 10 $\mu$M ouabain in the absence (A) and presence (B) of 1 $\mu$M SEA0400. Expression of functional NCX in the cells observed was confirmed by the increase in intracellular $Ca^{2+}$ in response to low $Na^+$ solution.

*Effect of SEA0400 on ouabain-induced arrhythmia*

Effect of SEA0400 on ouabain-induced arrhythmia was examined in papillary muscles (Fig. 5). Application of 3 $\mu$M ouabain to papillary muscles induced positive inotropy; the contractile force at 10 min after the addition of ouabain increased to 272.7 ± 24.8% (n = 26) of that before the addition. This was followed by the appearance of arrhythmic contraction during the period between 10 and 60 min after ouabain application in 19 out of 26 preparations. The arrhythmic contractions were larger than the stimulation-evoked periodic contractions. After 20 min, oscillatory aftercontractions with decremental amplitude were observed instead of the large arrhythmic contractions. In addition to these changes, 3 $\mu$M ouabain induced contracture; the basal tension at 30 min after the addition of ouabain was 305.0 ± 67.1% (n = 26) of the contractile force in the absence of ouabain.

In the presence of 1 $\mu$M SEA0400, the ouabain-induced positive inotropy was smaller than that in the absence of SEA0400; contractile force at 10 min was 239 ± 22.7% (n = 26) of that before ouabain addition. The arrhythmic contraction during the period between 10 and 60 min was observed in 12 out of 26 preparations

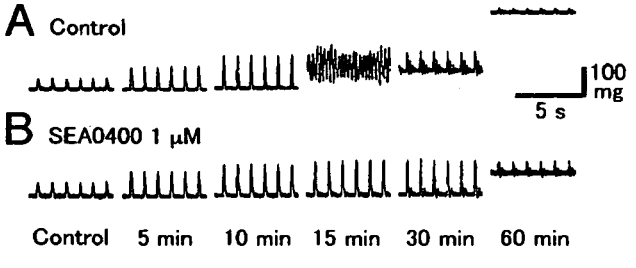


**Fig. 5.** Effect of SEA0400 on ouabain-induced arrhythmogenesis. Typical records of the contractile response of papillary muscles to 3 $\mu$M ouabain in the absence (A) and presence (B) of 1 $\mu$M SEA0400. Note that SEA0400 inhibited arrhythmic contractions and reduced the elevation of basal tension.

in the presence of SEA0400; the incidence was significantly smaller than in the absence of SEA0400. The oscillatory aftercontractions observed after 20 min were not inhibited by SEA0400 but the elevation of basal tension was significantly reduced by SEA0400. The

basal tension at 30 min after the addition of ouabain in the presence of SEA0400 was 184.8 ± 55.5% (n = 26) of the contractile force in the absence of ouabain.

## Discussion

In isolated guinea-pig papillary muscles, SEA0400 reduced the contracture induced by a low-sodium solution (Fig. 1) indicating that it could inhibit $Ca^{2+}$ influx through NCX not only in cardiomyocytes (7), but also in myocardial tissue. SEA0400 also attenuated the elevation of basal tension during late experimental ischemia (16), which is considered to reflect the inhibition of $Ca^{2+}$ influx through the reverse mode NCX. SEA0400 produced concentration-dependent positive inotropy in mouse ventricular myocardium (11). When the effect of SEA0400 on NCX was examined in voltage clamped guinea-pig ventricular myocytes, SEA0400 inhibited both forward and reverse modes with the same potency (7). SEA0400 increased the contractile force of guinea-pig papillary preparations, suggesting that SEA0400 inhibits $Ca^{2+}$ extrusion through the forward mode NCX in tissue preparations. However, the effect of NCX inhibition by SEA0400 on the forward and reverse modes may not be the same in tissue preparations where the membrane potential and ionic conditions change during the action potential cycle.

Concerning species difference in the positive inotropic effect, SEA0400 (1 $\mu$M) increased the contractile force of papillary muscle preparations by only 5% (present study) or less (16) in the guinea pig, but by 25% in the mouse (11). In the guinea-pig ventricle, the membrane potential is more negative than the equilibrium potential of NCX only during the resting period when the intracellular $Ca^{2+}$ is low. In contrast, the mouse has a short duration and higher intracellular $Na^+$ concentration, which favors $Ca^{2+}$ extrusion through the forward mode NCX during early diastole when the intracellular $Ca^{2+}$ is still elevated (1). Thus, NCX inhibition would result in larger positive inotropy in the mouse ventricle, where the functional role of $Ca^{2+}$ extrusion through the forward mode NCX is larger. Ouabain treatment of the guinea-pig ventricle, which increases intracellular $Na^+$ concentration, would enhance $Ca^{2+}$ influx from the reverse mode NCX. There is a report that inhibition of NCX by SEA0400 is more potent under higher intracellular $Na^+$ concentration (21). This may also partially underlie the difference in positive inotropy by SEA0400 between the guinea pig and mouse, which has a higher intracellular $Na^+$ concentration (22).

SEA0400 significantly reduced the ouabain-induced positive inotropy (Fig. 2), indicating that NCX activity is essential for ouabain action. Inhibition of inotropy induced by a higher concentration (3 $\mu$M) of ouabain was smaller (Fig. 5), probably because the inhibition of NCX is not complete (about 80%) with 1 $\mu$M SEA0400 (7). SEA0400 had no effect on IBMX-induced inotropy (Fig. 3), which reflects its high NCX specificity. Reduction of ouabain-induced inotropy by SEA0400 also suggests that the NCX is at least partly operating in the reverse mode in the presence of ouabain. Reduction of low-sodium contracture by SEA0400 indicated that it could inhibit $Ca^{2+}$ influx through NCX not only in cardiomyocytes (7) but also in myocardial tissue. That ouabain can activate $Ca^{2+}$ influx through reverse mode NCX was futher confirmed by induction of rise in intracellular $Ca^{2+}$ concentration in HEK293 cells expressing the cardiac type NCX (Fig. 4). Thus, the present results provide pharmacological evidence for a contribution of the reverse mode NCX activity in the cardiac glycoside-induced inotropy. However, other mechanisms such as stimulation of sarcoplasmic reticulum (SR) $Ca^{2+}$ release have also been postulated (23). The present results do not exclude such possibilities. Rather, inhibition of the NCX pathway by the highly specific inhibitor SEA0400 would be a useful strategy to clarify the additional mechanisms for cardiac glycoside-induced inotropy.

Ouabain has been considered to increase intracellular $Na^+$ concentration, shift the balance of the two modes of NCX to favor the reverse mode, and increase cellular $Ca^{2+}$ load. When this $Ca^{2+}$ load exceeds the capacity of the SR, abnormal $Ca^{2+}$ release from the SR occurs, which in turn triggers abnormal electrical activity and arrhythmic contractions. In the present study, the ouabain-induced increase in basal tension and arrhythmic contractions were significantly reduced by SEA0400 (Fig. 5). This provides pharmacological evidence that NCX plays a crucial role in ouabain-induced arrhythmogenesis. It was also reported that SEA0400 attenuated ouabain-induced arrhythmia in a canine in vivo model (18) and in isolated Purkinje fibers (24). The effect of SEA0400 on other types of arrhythmia has also been investigated. Attenuation of arrhythmia induced by ischemia-reprefusion was shown to be attenuated by SEA0400 in the in vitro rat (13) and guinea-pig (16) model. On the other hand, SEA0400 was reported to be ineffective against various aconitine-induced arrhythmia models in the guinea pig (25). We have reported that KB-R7943, a less selective NCX inhibitor, inhibits aconitine-induced intracellular $Ca^{2+}$ oscillations in isolated rat ventricular myocytes (26), which may reflect the action of KB-R7943 on ion channels other than the NCX (7).

In conclusion, the present results provide pharmaco-

logical evidence that the $Na^+/Ca^{2+}$ exchanger is involved in ouabain-induced inotropy and arrhythmogenesis. SEA0400 may be promising as a therapeutic agent against arrhythmia dependent on NCX function.

## Acknowledgments

This study was supported in part by a grant-in-aid for Drug Innovation Science Project to T.K. and K.S. from the Japan Health Science Foundation. This study was performed as a part of the project "Research on the molecular mechanisms of appearance of age-related diseases by failure of cell function control system, and their prevention and treatment" by the "Research Center for Aging and Age related Diseases" established in the Toho University Faculty of Pharmaceutical Sciences.

## References

1 Bers D. Cardiac $Na^+/Ca^{2+}$ exchange function in rabbit, mouse and man: what's the difference? J Mol Cell Cardiol. 2002;34:369–373.

2 Bers D. Cardiac myocytes $Ca^{2+}$ and $Na^+$ regulation in normal and failing hearts. J Pharmacol Sci. 2006;100:315–322.

3 Maltsev VA, Vinogradova TM, Lakatta EG. The emergence of a general theory of the initiation and strength of the heartbeat. J Pharmacol Sci. 2006;100:338–369.

4 Levi A, Boyett M, Lee C. The cellular actions of digitalis glycosides on the heart. Prog Biophys Mol Biol. 1994;62:1–54.

5 Reuter H, Henderson S, Han T, Ross R, Goldhaber J, Philipson K. The $Na^+$-$Ca^{2+}$ exchanger is essential for the action of cardiac glycosides. Circ Res. 2002;22:305–308.

6 Matsuda T, Arakawa N, Takuma K, Kishida Y, Kawasaki Y, Sakaue M, et al. SEA0400, a novel and selective inhibitor of the $Na^+$-$Ca^{2+}$ exchanger, attenuates reperfusion injury in the in vitro and in vivo cerebral ischemic models. J Pharmacol Exp Ther. 2001;298:249–256.

7 Tanaka H, Nishimaru K, Aikawa T, Hirayama W, Tanaka Y, Shigenobu K. Effect of SEA0400, a novel inhibitor of sodium-calcium exchanger, on myocardial ionic currents. Br J Pharmacol. 2002;135:1096–1100.

8 Iwamoto T. Forefront of $Na^+/Ca^{2+}$ exchanger studies: molecular pharmacology of $Na^+/Ca^{2+}$ exchange inhibitors. J Pharmacol Sci. 2004;96:27–32.

9 Matsuda T, Koyama Y, Baba A. Functional proteins involved in regulation of intracellular $Ca^{2+}$ for drug development: pharmacology of SEA0400, a specific inhibitor of the $Na^+$-$Ca^{2+}$ exchanger. J Pharmacol Sci. 2005;97:339–343.

10 Namekata I, Kawanishi T, Iida-Tanaka N, Tanaka H, Shigenobu K. Quantitative fluorescence measurement of cardiac $Na^+/Ca^{2+}$ exchanger inhibition by kinetic analysis in stably transfected HEK293 cells. J Pharmacol Sci. 2006;101:356–360.

11 Tanaka H, Namekata I, Takeda K, Kazama A, Shimizu Y, Moriwaki R, et al. Unique excitation-contraction characteristics of mouse myocardium as revealed by SEA0400, a specific inhibitor of $Na^+/Ca^{2+}$ exchanger. Naunyn-Schmiedebergs Arch Pharmacol. 2005;371:526–534.

12 Ogata M, Iwamoto T, Tazawa N, Nishikawa M, Yamashita J, Takaoka M, et al. A novel and selective $Na^+/Ca^{2+}$ exchange inhibitor, SEA0400, improves ischemia/reperfusion-induced renal injury. Eur J Pharmacol. 2003;478:187–198.

13 Takahashi K, Takahashi T, Suzuki T, Onishi M, Tanaka Y, Hamano-Takahashi A, et al. Protective effects of SEA0400, a novel and selective inhibitor of the $Na^+/Ca^{2+}$ exchanger, on myocardial ischemia-reperfusion injuries. Eur J Pharmacol. 2003;458:155–162.

14 Magee W, Deshmukh G, Deninno M, Sutt J, Chapman J, Tracey W. Differing cardioprotective efficacy of the $Na^+/Ca^{2+}$ exchanger inhibitors SEA0400 and KB-R7943. Am J Physiol Heart Circ Physiol. 2003;284:H903–H910.

15 Yoshiyama M, Nakamura Y, Omura T, Hayashi T, Takagi Y, Hasegawa T, et al. Cardioprotective effect of SEA0400, a selective inhibitor of the $Na^+/Ca^{2+}$ exchanger, on myocardial ischemia-reperfusion injury in rats. J Pharmacol Sci. 2004;95: 196–202.

16 Namekata I, Nakamura H, Shimada H, Tanaka H, Shigenobu K. Cardioprotection without cardiosuppression by SEA0400, a novel inhibitor of $Na^+$-$Ca^{2+}$ exchanger, during ischemia and reperfusion in guinea-pig myocardium. Life Sci. 2005;77:312–324.

17 Namekata I, Shimada H, Kawanishi T, Tanaka H, Shigenobu K. Reduction by SEA0400 of myocardial ischemia-induced cytoplasmic and mitochondrial $Ca^{2+}$ overload. Eur J Pharmacol. 2006;543:108–115.

18 Nagasawa Y, Zhu B, Chen J, Kamiya K, Miyamoto S, Hashimoto K. Effects of SEA0400, a $Na^+/Ca^{2+}$ exchange inhibitor, on ventricular arrhythmias in the in vivo dogs. Eur J Pharmacol. 2005;506:249–255.

19 Agata N, Tanaka H, Shigenobu K. Developmental changes in action potential properties of guinea-pig myocardium. Acta Physiol Scand. 1993;149:331–337.

20 Mukai M, Terada H, Sugiyama S, Satoh H, Hayashi H. Effects of a selective inhibitor of $Na^+/Ca^{2+}$ exchange, KB-R7943, on reoxygenation-induced injuries in guinea pig papillary muscles. J Cardiovasc Pharmacol. 2000;35:121–128.

21 Lee C, Visen N, Dhalla N, Le H, Isaac M, Choptiany P, et al. Inhibitory profile of SEA0400 [2-[4-[(2,5-difluorophenyl) methoxy]phenoxy]-5-ethoxyaniline] assessed on the cardiac $Na^+$-$Ca^{2+}$ exchanger, NCX1.1. J Pharmacol Exp Ther. 2004; 311:748–757.

22 Yao A, Su Z, Nonaka A, Zubair I, Lu L, Philipson KD, et al. Effects of overexpression of the $Na^+$-$Ca^{2+}$ exchanger on $[Ca^{2+}]$I transients in murine ventricular myocytes. Circ Res. 1998; 82:657–665.

23 Nishio M, Ruch S, Kelly J, Aistrup G, Sheehan K, Wasserstrom J. Ouabain increases sarcoplasmic reticulum calcium release in cardiac myocytes. J Pharmacol Exp Ther. 2003;308:1181–1190.

24 Nagy Z, Virag L, Toth A, Biliczki P, Acsai K, Banyasz T, et al. Selective inhibition of sodium-calcium exchanger by SEA-0400 decreases early and delayed after depolarization in canine heart. Br J Pharmacol. 2004;143:827–831.

25 Amran S, Hashimoto K, Homma N. Effects of sodium-calcium exchange inhibitors, KB-R7943 and SEA0400, on aconitine-induced arrhythmias in guinea pigs in vivo, in vitro, and in computer simulation studies. J Pharmacol Exp Ther. 2004;310: 83–89.

26 Namekata I, Yamagishi R, Kato Y, Nakamura R, Tanaka H, Shigenobu K. Propagation of normal and abnormal cytoplasmic $Ca^{2+}$ oscillation into the cell nucleus in cardiomyocytes. Bioimages. 2004;12:61–69.

*Pharmaceutical Research, Vol. 24, No. 9, September 2007 (© 2007)*
DOI: 10.1007/s11095-007-9296-2

*Research Paper*

# Significance of Local Mobility in Aggregation of β-Galactosidase Lyophilized with Trehalose, Sucrose or Stachyose

**Sumie Yoshioka,[1,2] Tamaki Miyazaki,[1] Yukio Aso,[1] and Tohru Kawanishi[1]**

*Received January 3, 2007; accepted March 14, 2007; published online April 3, 2007*

***Purpose.*** The purpose of this study is to compare the effects of global mobility, as reflected by glass transition temperature ($T_g$) and local mobility, as reflected by rotating-frame spin-lattice relaxation time ($T_{1\rho}$) on aggregation during storage of lyophilized β-galactosidase (β-GA).
***Materials and Methods.*** The storage stability of β-GA lyophilized with sucrose, trehalose or stachyose was investigated at 12% relative humidity and various temperatures (40–90°C). β-GA aggregation was monitored by size exclusion chromatography (SEC). Furthermore, the $T_{1\rho}$ of the β-GA carbonyl carbon was measured by $^{13}C$ solid-state NMR, and $T_g$ was measured by modulated temperature differential scanning calorimetry. Changes in protein structure during freeze drying were measured by solid-state FT-IR.
***Results.*** The aggregation rate of β-GA in lyophilized formulations exhibited a change in slope at around $T_g$, indicating the effect of molecular mobility on the aggregation rate. Although the $T_g$ rank order of β-GA formulations was sucrose < trehalose < stachyose, the rank order of β-GA aggregation rate at temperatures below and above $T_g$ was also sucrose < trehalose < stachyose, thus suggesting that β-GA aggregation rate is not related to ($T-T_g$). The local mobility of β-GA, as determined by the $T_{1\rho}$ of the β-GA carbonyl carbon, was more markedly decreased by the addition of sucrose than by the addition of stachyose. The effect of trehalose on $T_{1\rho}$ was intermediate when compared to those for sucrose and stachyose. These findings suggest that β-GA aggregation rate is primarily related to local mobility. Significant differences in the second derivative FT-IR spectra were not observed between the excipients, and the differences in β-GA aggregation rate observed between the excipients could not be attributed to differences in protein secondary structure.
***Conclusions.*** The aggregation rate of β-GA in lyophilized formulations unexpectedly correlated with the local mobility of β-GA, as indicated by $T_{1\rho}$, rather than with ($T-T_g$). Sucrose exhibited the most intense stabilizing effect due to the most intense ability to inhibit local protein mobility during storage.

**KEY WORDS:** β-galactosidase; global mobility; local mobility; lyophilized formulation; solid-state stability.

## INTRODUCTION

Close correlations between storage stability and molecular mobility have been demonstrated for various lyophilized formulations of peptides and proteins (1,2). Aggregation between protein molecules is a degradation pathway commonly observed in lyophilized protein formulations. The rate of protein aggregation is generally considered to depend on the translational mobility of protein molecules, which is related to structural relaxation (α-relaxation) of the formulation. Correlations between aggregation rates and structural relaxation have been shown in various protein systems in visible ways, such as enhancement of aggregation associated with decreases in glass transition temperature ($T_g$) (3–6) and changes in the temperature dependence of aggregation rates around $T_g$ (7–10). However, recent studies have suggested that molecular mobility with a length scale shorter than structural relaxation (β-relaxation or local mobility), rather than structural relaxation, is critical to protein aggregation (11,12).

The rate of protein aggregation in lyophilized formulations is also affected by the degree of change in protein conformation produced during the freeze-drying process (1). Greater changes in protein conformation are considered to lead to enhanced aggregation during subsequent storage.

In this study, the significance of local mobility in aggregation of lyophilized β-galactosidase (β-GA), a model protein, is discussed in comparison with the significance of structural relaxation and conformational changes. β-GA underwent significant inactivation during freeze drying with dextran, thus suggesting that significant conformational changes occurred during the process (13). When freeze dried with polyvinylalcohol or methylcellulose, inactivation was not observed during freeze drying (10). However, the time

[1] Division of Drugs, National Institute of Health Sciences, 1-18-1 Kamiyoga, Setagaya-ku, Tokyo 158-8501, Japan.
[2] To whom correspondence should be addressed. (e-mail: yoshioka@nihs.go.jp)

0724-8741/07/0900-1660/0 